Synthesis and Anti-Picornaviridae *In Vitro* Activity of a New Class of Helicase Inhibitors the *N*,*N*'-bis[4-(1*H*(2*H*)-benzotriazol-1(2)-yl)phenyl] alkyldicarboxamides

A. Carta[a,*], M. Loriga[a], S. Piras[a], G. Paglietti[a], M. Ferrone[b], M. Fermeglia[b], S. Pricl[b], P. La Colla[c,*], G. Collu[c], T. Sanna[c] and R. Loddo[c]

[a]*Dipartimento Farmaco Chimico Tossicologico, via Muroni 23/a, 07100 Sassari, Italy,* [b]*Laboratorio MOSE, Dipartimento di Ingegneria Chimica, Piazzale Europa 1, 34127 Trieste, Italy,* [c]*Dipartimento di Scienze e Tecnologie Biomediche, Sezione di Microbiologia e Virologia Generale e Biotecnologie Microbiche, Università degli Studi di Cagliari, Cittadella Universitaria, 09042 Monserrato (Cagliari), Italy*

Abstract: A series *N*,*N*'-bis[4-(1*H*(2*H*)-benzotriazol-1(2)-yl)phenyl]alkyldicarboxamides (**3a-f** and **5a-j**) were prepared starting from their already known (**1a-d**) and (**4a-c**) or new (**4d**) amine parents. Because of the antiviral activity of several *N*-[4-(1*H*(2*H*)-benzotriazol-1(2)-yl)phenyl]alkylcarboxamides previously reported, title compounds were evaluated *in vitro* for cytotoxicity and antiviral activity against viruses representative of *Picornaviridae*, [i.e. *Enterovirus* Coxsackie B2 (CVB-2) and Polio (Sb-1)] and of two of the three genera of the *Flaviviridae* [Bovine Viral Diarrhea Virus (BVDV) and Yellow Fever Virus (YFV)]. Furthermore, because of the *in silico* activity against the RNA-dependent RNA-helicase of Polio 1 previously reported, title compounds were evaluated against the 3D model of the Sb-1 helicase and against the 2D model of the CVB-2 helicase. As a reference we used the antiviral and *in silico* activities of an imidazo counterpart of the title compounds, *N*,*N*'-bis[4-(2-benzimidazolyl)phenyl]alkyldicarboxamides (**III**) that other authors reported to be able to inhibit the corresponding enzyme of Hepatitis C Virus (HCV). In cell-based antiviral assays, *N*,*N*'-bis[4-(1*H*-benzotriazol-1-yl)phenyl]alkyldicarboxamides (**3a-f**) resulted completely inactive whereas the bis-5,6-dimethyl-benzotriazol-2-yl derivatives (**5d-f**) exhibited good activity against the *Enteroviruses*, (EC_{50}s ranged between 7 and 11 μM against CVB-2 and 19-52 against Sb-1). Interestingly, bis-5,6-dichloro-benzotriazol-2-yl derivatives (**5h-j**) showed very selective activity against CVB-2 (EC_{50}s = 4-11 μM) whereas they resulted completely inactive against all the other viruses screened. In general, all title compounds showed a good cytotoxicity profile in MT-4 cells. Molecular modeling investigations showed that active compounds may interact with the binding site of the Sb-1 helicase and that their free binding energy values are in agreement with their EC_{50}s values.

Key Words: Benzotriazol-1(2)-yl-phenylalkyldicarboxamides, anti-viral activity, picornaviridae, flaviviridae, helicase, *in silico* evaluation, cytotoxicity, SAR.

INTRODUCTION

The viruses belonging to the family Picornaviridae (picornaviruses), all having a single-stranded positive-sense RNA ($ssRNA^+$) genome, cause a dramatic variety of illnesses, including: meningitis, colds, heart infection, conjunctivitis, and hepatitis. [Different viruses produce different clinical outcomes, while the same types may cause different manifestations in different individuals.]. After the infection, the host cell protein synthesis declines precipitously. A virus-coded, RNA-dependent, RNA polymerase copies the genome producing negative-sense RNA strands, which serve as templates for the synthesis of positive-sense RNAs.

Picornaviridae includes 9 genera, 3 of which are human pathogens: *Enterovirus* (containing poliovirus, enterovirus, coxsackievirus, echovirus), *Rhinovirus* (approximately 105 serotypes), and *Hepatovirus* (hepatitis A virus [HAV]).

*Address correspondence to these authors at the Dipartimento Farmaco Chimico Tossicologico, via Muroni 23/a, 07100 Sassari, Italy; Tel: +39-079-228722; Fax: +39-079-228720; E-mail: acarta@uniss.it

Dipartimento di Scienze e Tecnologie Biomediche, Sezione di Microbiologia e Virologia Generale e Biotecnologie Microbiche, Università degli Studi di Cagliari, Cittadella Universitaria, 09042 Monserrato (Cagliari), Italy; E-mail: placolla@unica.it

At present, no specific antiviral therapy is available for the treatment of Picornaviridae infections.

Recently we reported the synthesis and anti-viral screening of a series of *N*-[4-(1*H*(2*H*)-benzotriazol-1(2)-yl)phenyl] alkylcarboxamides [1]. In particular, two of them emerged for their selective activity against representative Enterovirus: i. e. compounds (**I**) and (**II**), active against Coxsackie Virus B (CVB-2) (EC_{50} = 10 μM) and Polio Virus (Sb-1) (EC_{50} = 30 μM), respectively. Furthermore, molecular dynamics simulations on *N*-[4-(1*H*(2*H*)-benzotriazol-1(2)-yl)phenyl] alkylcarboxamides/Polio helicase complexes have shown the affinities of compounds (**I** and **II**). The structure of **I** and **II** are reported in Fig. (**1**).

In a 1997 patent, Diana *et al.* reported that some *N*,*N*'-bis [4-(2-benzimidazolyl)phenyl]alkyldicarboxamides were able to inhibit the RNA-dependent RNA-helicase of Hepatitis C Virus (HCV) by IC_{50} of 0.7 μM [2]. One of these derivatives, compound **III**, is reported in Fig. (**2**).

Based on these premises, we have now prepared a series of *N*,*N*'-bis[4-(1*H*(2*H*)-benzotriazol-1(2)-yl)phenyl]alkyldicarboxamides (**3a-f** and **5a-j**), summarized in Fig. (**3**), with the aim of verifying whether the replacement of benzimida-

1573-4064/07 $50.00+.00

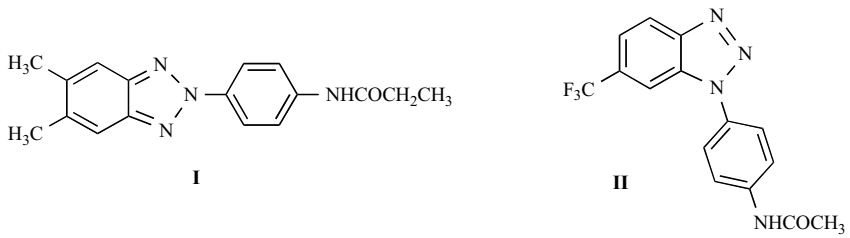

Fig. (1). Benzotriazolyl-phenyl-alkylcarboxamides anti CVB-2 (**I**) and anti SB-1 (**II**).

zole with benzotriazole could lead to improvment of the antiviral activity. As a reference, compound **III** was re-synthesized and evaluated for antiviral activity. Title compounds and the benzimidazole derivative (**III**) were compared *in silico* for their binding mode to the Sb-1 helicase, and were evaluated in cell-based assays against the above cited Enteroviruses, CVB-2 and Sb-1, and against BVDV and YFV, two positive-stranded RNA viruses usually used *in vitro* as surrogates of HCV.

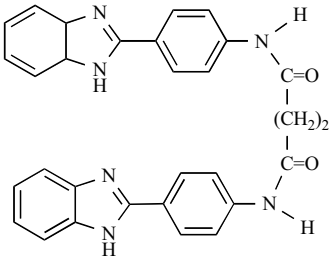

III

Fig. (2). The inhibitor of the HCV RNA-dependent RNA-helicase *N*,*N*'-bis[4-(2-benzimidazolyl)phenyl]succinylcarboxamides (**III**).

Furthermore, the cytotoxicity of title compounds and **III** was evaluated also in exponentially growing MT-4 cells, a lymphoblastoid cell line growing in suspension cultures.

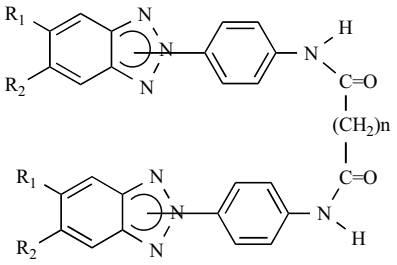

3a-f and **5a-j**

Fig. (3). *N*,*N*'-bis[4-(1*H*(2*H*)-benzotriazol-1(2)-yl)-phenyl]alkyldicarboxamides (**3a-f** and **5a-j**).

CHEMISTRY

The *N*,*N*'-bis[4-(1*H*(2*H*)-benzotriazol-1(2)-yl)phenyl]alkyldicarboxamides (**3a-f** and **5a-j**) were prepared, as reported in Scheme (**1**), by condensation of the amines 1-(4-aminophenyl)benzotriazoles (**1a-d**) and 2-(4-aminophenyl)benzotriazoles (**4a-d**) with the suitable diacyl dichlorides in dimethylformamide (DMF) in the presence of triethylamine (TEA). After elimination of the triethylamine hydrochloride (Et_3N,HCl), the solid crude obtained was purified by crystallization with methanol or chromatography on silica gel.

Amines (**1a-d** and **4a-c**) were previously described [1] while 4d was prepared, as reported in Scheme (**2**), by condensation of 5,6-dichlobenzotriazole (7) with 4-chloronitrobenzene (8) in DMF in the presence of KOH, to obtain an isomeric mixture of 1(2)-p-nitrophenyl derivatives (**9a,b**). The latter underwent simultaneous reduction with methylhydrazine in ethanol, heated in a sealed steel vessel at 100 °C for 80 h. Isolation of the single isomers 1e and 4d was performed on silica gel column chromatography (eluent: light petroleum-ethyl acetate 7:3). Attempts of reduction of the nitroderivatives (**9a,b**) by hydrogenation in a Parr apparatus, or with hydrazine in refluxing ethanol, using 10% palladium-charcoal as catalyst, afforded mixture of 1e and 4d along with their known dehalogenated derivatives 1(2)-(4-aminophenyl)benzotriazoles (**10a,b**) [1]. *N*,*N*'-bis[4-(2-benzimidazolyl)phenyl]succinylcarboxamide (III) was prepared according to the procedure described by Diana *et al.* [2].

VIROLOGY

Title compounds (**3a-f** and **5a-j**) were evaluated *in vitro* against the *Enteroviruses* Coxsackie B2 (CVB-2) and Polio (Sb-1)] and against representatives of two of the three genera of the Flaviviridae family, i.e. *Flaviviruses* (Yellow Fever Virus, YFV) and *Pestiviruses* (Bovine Viral Diarrhea Virus, BVDV), as *Hepaciviruses* do not replicate in cell cultures.

MOLECULAR MODELING STUDY

Title compounds (**3a-f**, **5a-j)** and benzimidazole derivative (**III**) were evaluated *in silico* for their binding mode versus the Polio virus (Sb-1) helicase. The protein 3D model was obtained in our previous work [1] by homology modeling techniques, as the corresponding crystal structure is not currently available in the Protein data Bank. All the compounds were modeled and docked into the protein, and the corresponding free energies of binding were calculated using molecular dynamics simulations. Unfortunately, homology standard techniques were not able to produce a reliable 3D model for the Coxsackie B2 (CVB-2) virus helicase, due to very low sequence identities found during alignment processes. Accordingly, the protein 3D model is currently being constructed using ab initio methods.

RESULTS AND DISCUSSION

N,*N*'-bis[4-(1*H*(2*H*)-benzotriazol-1(2)-yl)phenyl]alkyldicarboxamides (**3a-f** and **5a-j**) were evaluated, and the results are reported in Table (**3**), in parallel cell-based assays for cytotoxicity and antiviral activity in comparison with the

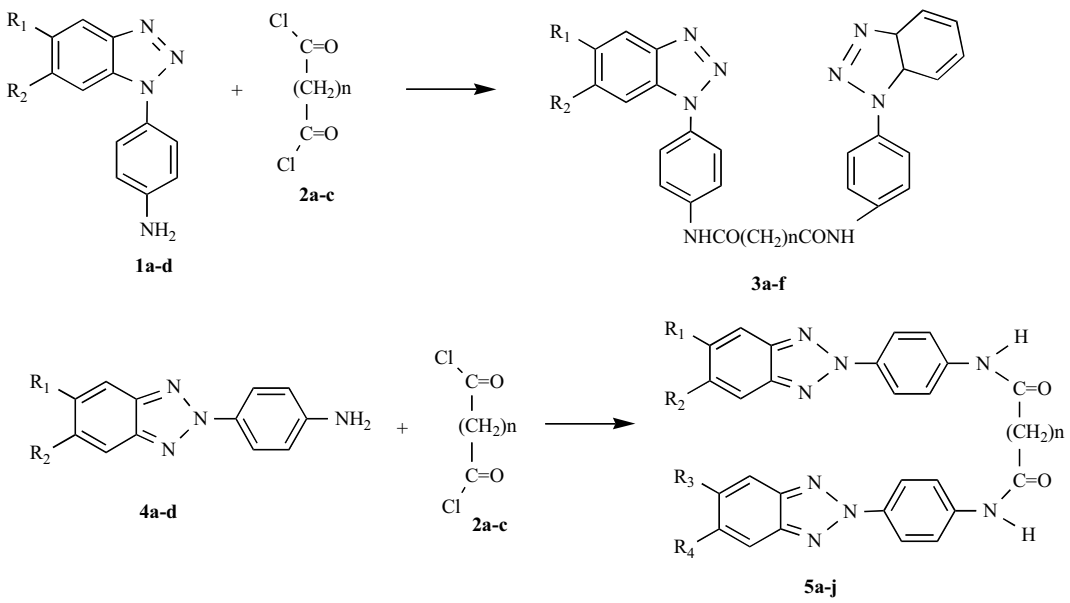

Scheme 1. Synthesis of *N*,*N*'-bis[4-(1*H*(2*H*)-benzotriazol-1(2)-yl)phenyl]alkyldicarboxamides (**3a-f** and **5a-j**).

previous synthesized benzotriazolic monomer derivatives (**I** and **II**) and with the benzimidazolic dimer derivative *N*,*N*'-bis[4-(2-benzimidazolyl)phenyl]succinylcarboxamides (**III**). As reported in Table (**2**), all compounds showed no cytotoxicity against confluent cell monolayers (in stationary growth) used for the various antiviral activity. For this reason, the cytotoxicity was evaluated against exponentially growing lymphoblastoid MT-4 cells.

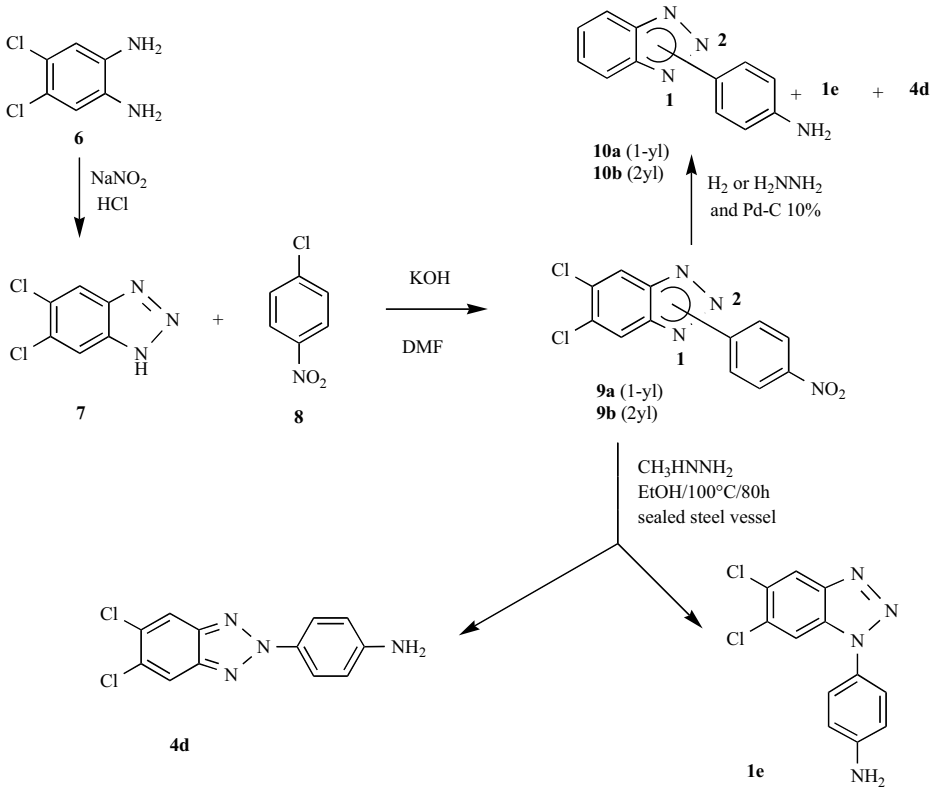

Scheme 2. Synthesis of intermediate (**4d**).

Table 1. Substituents of Scheme 1

Compds	R_1	R_2	n	Compds	R_1	R_2	n
1a	H	H	-	**4a**	H	H	-
1b	CH_3	CH_3	-	**4b**	CH_3	CH_3	-
1c	CF_3	H	-	**4c**	CF_3	H	-
1d	H	CF_3	-	**4d**	Cl	Cl	
1e	Cl	Cl	-	**5a**	H	H	2
2a	-	-	2	**5b**	H	H	3
2b	-	-	3	**5c**	H	H	4
2c	-	-	4	**5d**	CH_3	CH_3	2
3a	H	H	2	**5e**	CH_3	CH_3	3
3b	H	H	3	**5f**	CH_3	CH_3	4
3c	H	H	4	**5g**	CF_3	H	2
3d	CH_3	CH_3	2	**5h**	Cl	Cl	2
3e	CF_3	H	2	**5i**	Cl	Cl	3
3f	H	CF_3	2	**5j**	Cl	Cl	4

Table 2. Cytotoxicity of Reference Compounds I, II and III and Benzotriazolodicarboxamides 3a-f, and 5a-g

Compds	Cell lines			
	[a]CC_{50}			[b]CC_{50}
	[c]MDBK	[d]BHK	[e]Vero	[f]MT-4
I	>100	>100	>100	≥100
II	>100	>100	>100	55
III	>100	>100	>100	100
3a	>100	>100	>100	>100
3b	>100	>100	>100	50
3c	>100	>100	>100	>100
3d	>100	>100	>100	≥100
3e	68	>100	>100	≥100
3f	>100	>100	>100	≥100
5a	>100	>100	>100	>100
5b	>100	>100	>100	>100
5c	>100	>100	>100	>100
5d	>100	≥100	>100	≥100
5e	>100	>100	>100	≥100
5f	>100	>100	>100	42
5g	75	56	>100	≥100

(Table 2. Contd….)

Compds	Cell lines			
	[a]CC_{50}			[b]CC_{50}
	[c]MDBK	[d]BHK	[e]Vero	[f]MT-4
5h	>100	>100	≥100	>100
5i	>100	>100	≥100	>100
5j	>100	>100	≥100	>100

[a]Compound concentration (μM) required to reduce the viability of mock-infected cells by 50%, as determined by the MTT method, or the confluency of the monolayer (Vero), as determined by methylene blue staining.

[b]Compound concentration (μM) required to reduce cell proliferation by 50%, as determined by the MTT method, under conditions allowing untreated controls to undergo at least three consecutive rounds of multiplication. Data represent mean values for three independent determinations. Variation among duplicate samples was less than 15%.

[c]Madin Darby Bovine Kidney; [d]Baby Hamster Kidney; [e]Monkey Kidney; [f]$CD4^+$ human T-cells.

Table 3. Activity of Reference Compounds I, II and III and Benzotriazolodicarboxamides 3a-f, and 5a-g, Against the RNA Viruses Indicated

Compds	CVB-2 [b]EC_{50}	Sb-1 [b]EC_{50}	BVDV [a]EC_{50}	YFV [b]EC_{50}	Compds	CVB-2 [b]EC_{50}	Sb-1 [b]EC_{50}	BVDV [a]EC_{50}	YFV [b]EC_{50}
I	10	>100	>100	>100	**5b**	>100	>100	>100	>100
II	>90	30	>100	>100	**5c**	33	>100	>100	>100
III	50	>100	>100	>100	**5d**	11	52	>100	>100
3a	>100	>100	>100	>100	**5e**	8	43	>100	>100
3b	>100	>100	>100	>100	**5f**	7	19	>100	82
3c	>100	>100	>100	>100	**5g**	38	100	>75	>56
3d	>100	>100	>100	>100	**5h**	4	>100	>100	>100
3e	>100	>100	>68	>100	**5i**	11	>100	>100	>100
3f	>100	>100	>100	>100	**5j**	9	>100	88	>100
5a	>100	>100	>100	>100					

[a]Compound concentration (μM) required to achieve 50% protection from virus-induced cytopathogenicity, as determined by the MTT method.

[b] Compound concentration (μM) required to reduce the virus plaque number by 50%.

As far as the antiviral activity was concerned, none of the compounds of the series **3** (*N*,*N*'-bis[4-(1*H*-benzotriazol-1-yl)phenyl]alkyldicarboxamides) protected the cells from the cytopathogenicity induced by the representative RNA viruses tested. On the other hand, compounds of the series **5** (*N*,*N*'-bis[4-(2*H*-benzotriazol-2-yl)phenyl]alkyldicarboxamides) bearing substituents on benzene-moiety (**5d-j**) exhibited the best activity against the *Enteroviruses* tested (see Table **3**). The EC_{50}s were ranged between 4 and 38 μM against CVB-2 (**5d-j**) and 19-52 μM against Sb-1 (**5d-f**). In general the compounds which were unsubstituted or bearing trifluoromethyl group on the benzotriazole-moiety (**5a-c**) were poorly active or inactive. Furthermore, compounds **5d-f** exhibited good activity against both CVB-2 and Sb-1, while **5h-j** were electively active only against CVB-2. These observations are in agreement with the data reported for the monomeric series, in fact, in spite of their lower activity 5(6)-substituted-benzotriazol-2-yl monomers were in general the most active against both CVB-2 and Sb-1. Introduction of two chorine atoms on the benzo-moiety allowed to improve the activity against CVB-2. Furthermore, the size of the spacer between the two monomers (2, 3 or 4 atoms of carbon linked to the two carbonyl groups) seem to be not particularly relevant for the activity. Unexpectedly, the dimeric reference compound **III** (*N*,*N*'-bis[4-(2-benzimidazolyl)phenyl]succinylcarboxamide) resulted completely inactive against BVDV, YFV and Sb-1, and only moderate active against CVB-2. Interestingly, compounds **5f** and **5j** were the only new derivatives which showed moderate activity against YFV (EC_{50} = 82 μM) and BVDV (EC_{50} = 88 μM) respectively.

According to the procedure adopted, all compounds were characterized by a similar docking mode in the putative binding site of the Polio (Sb-1) helicase, defined in our previous work [1]. This protein cavity is made up by two β-sheets, three helices, and three loops (see Fig. **4**). In particular, the residues lining the pocket include the side chains of residues Ser221, Thr222 and Asn223 (cyan), and residue Val127

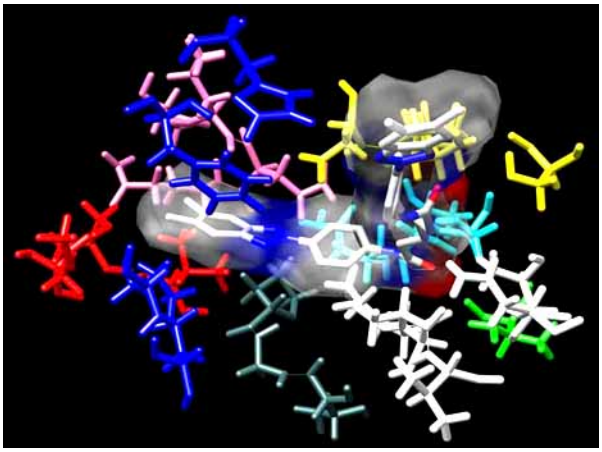

Fig. (4). Putative binding site for title compounds on Polio (Sb-1) helicase. Color legend: Ser221, Thr 222 and Asn223 (cyan), Val127 (green), Met293, Ser296, and Val299 (red), Lys135 to Val137 and Thr139 to Asn140 (white), Lys259, Ala263, Hys273, and Phe278 (blue) Asp177 to Gln180 (pink), Ser156 and Pro158 to Asp160 (yellow), and Pro131 to Thr133 (dark slate gray) (see text for more details). Compound 5f is depicted as an example in atom-colored stick representation (color code: C, light gray; N, blue; oxygen, red). Hydrogen atoms and water molecules have been omitted for clarity.

(green), yielding a contribution to binding from the two β-sheet portions. The portion of helix 1 involved encompasses residues Met293, Ser296, and Val299 (red), whilst helix 2 participates in ligand complexation with residues from Lys135 to Val137 and from Thr139 to Asn140 (white). Residues from helix 3 are Lys259, Ala263, Hys273, and Phe278 (blue). Finally, residues Asp177-Gln180 of the first loop (pink), Ser156 and Pro158-Asp160 of the second loop (yellow), and Pro131-Thr133 of the third loop constitute the remaining part of the binding pocket (dark slate gray).

Figure **5** shows 3D models of the **5f**/Polio (Sb-1) helicase complex. It is important to notice that, with respect to the previous series of compounds, i.e. *N*-[4-(1*H*(2*H*)-benzotriazol-1(2)-yl)phenyl]alkylcarboxamides, reported [1], all title compounds bind helicase Sb-1 in a different manner, as expected, due to their different shapes and dimensions. This is well quantified by the value of the solvent accessible volume of this new class of inhibitors, which on average has almost doubled with respect to that characterizing the previous molecular series (e.g., 1672 $Å^3$ vs. 891 $Å^3$, respectively). Accordingly, it is impossible for the protein pocket to host *N,N'*-bis[4-(1*H*(2*H*)-benzotriazol-1(2)-yl)phenyl]alkyldicarboxamides with the same binding mode, and the results form the docking study reveals that only one of the two identical inhibitors moieties can be positioned well within the binding pocket.

However, in correspondence of the most favored binding mode for the most active compounds, we observed the formation of a new, small network of H-bonds between **5f** and enzyme. In particular, the analysis of the trajectories of the MD simulations for the **5f**/helicase complex as an example indicates that there is a constant presence of an H-bond which involves the carbonyl oxygen atom of the Asn179 side

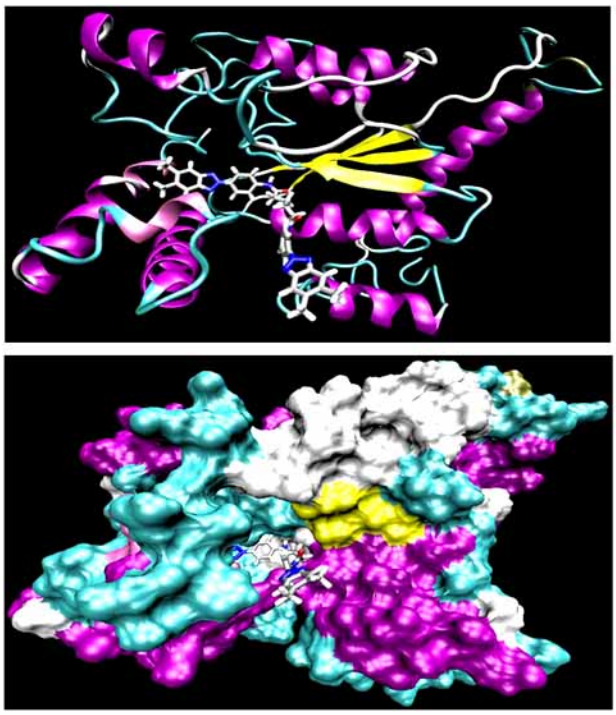

Fig. (5). Binding of compound **5f** to the putative binding site on the surface of Polio (Sb-1) helicase (top), and cartoon of the binding mode of compound **5f** in the putative binding site of the Polio (Sb-1) helicase (bottom). Compound **5f** is in atom-colored stick representation (color code: H, white; C, light gray; N, blue; O, red). Enzyme secondary structure motifs are colored as follows: α-helices, purple; β-sheets, yellow; coils and turns, cyan and white.

chain and the triazole N(1) atom of the drug, characterized by an average dynamic length (ADL) of 3.0 Å. At the same time, it is possible to verify the formation of other two H-bond interactions, the former between the C=O backbone group of Ser221 and the NH group of the amidic moiety of **5f** (ADL = 1.6 Å), and the latter between the carbonyl oxygen atom of the C=O group of the same amidic moiety of **5f** and the side chain hydroxyl group of Ser221 (ADL = 2.6 Å).

On the other hand, for the alternative complexes of the Polio (Sb-1) helicases with compounds **5a-c** and **5h-j**, respectively, we could observe only the formation of intermittent, shortly-lived H-bonds belonging to the network described above, whilst, in the case of the **3a-f** series of compounds, the H-bond network was never detected during the corresponding MD simulations. This is sensibly due to the peculiar conformation of these molecules induced by the bonds connecting the aromatic carbon and the triazolic N(1) atom, resulting in an overall poor binding mode.

Further insights and more quantitative information about the forces involved in substrate binding can be obtained by analyzing the values of the free energy component of binding, which are listed in Table (**4**) for the entire ligand compounds. Table (**4**) also reports the values obtained for the imidazo counterpart (**III**) for comparison. As we may see from this Table, both the intermolecular van der Waals and the electrostatics are important contributions to the binding.

Table 4. Free Energy Components and Total Binding Free Energies for Title Compounds

Compound	$\ddot{A}E_{ele}^{MM}$	$\ddot{A}E_{vdW}^{MM}$	ΔE_{MM}	$\ddot{A}G_{ele}^{sol}$	$\ddot{A}G_{np}^{sol}$	ΔG_{solv}	$T\Delta S$	ΔG_{bind}
III	-31.65	-41.98	-73.63	54.01	-7.70	-27.32	17.50	-9.82
3a	-30.12	-38.35	-68.47	54.11	-7.7	-22.06	17.30	-4.76
3b	-29.54	-38.67	-68.21	54.78	-7.4	-20.83	17.60	-3.23
3c	-29.78	-39.12	-68.90	54.87	-7.9	-21.93	19.20	-2.73
3d	-29.94	-39.89	-69.83	54.52	-7.9	-23.21	17.56	-5.65
3e	-31.51	-40.01	-71.52	56.70	-7.3	-22.12	18.30	-3.82
3f	-31.16	-39.42	-70.58	55.87	-7.2	-21.91	18.60	-3.31
5a	-32.12	-42.32	-74.44	53.77	-7.5	-28.17	16.90	-11.27
5b	-33.49	-42.01	-75.50	52.96	-7.6	-30.14	17.50	-12.64
5c	-32.36	-41.78	-74.14	53.06	-7.9	-28.98	17.20	-11.78
5d	-34.34	-44.64	-78.98	53.17	-7.8	-33.61	18.40	-15.21
5e	-34.99	-45.22	-80.21	52.75	-8.1	-35.56	18.00	-17.56
5f	-36.23	-45.87	-82.10	52.26	-8.0	-37.84	17.90	-19.94
5h	-33.31	-43.75	-77.06	57.65	-7.4	-26.81	18.30	-8.51
5i	-34.82	-44.04	-78.86	58.33	-7.6	-28.13	18.50	-9.63
5j	-33.73	-43.21	-76.94	56.89	-7.2	-27.25	17.90	-9.35

The electrostatic desolvation energy contribution generally disfavors the docking of ligand and enzyme. This is due to the unfavorable change in electrostatic solvation not fully compensated by the complexes formation, yielding a negative net electrostatic contribution to the binding. Indeed, from Table (**4**), in all cases the association between inhibitors and Sb-1 helicase is mainly driven by more favorable nonpolar interactions in the complex than in solution. This result can be determined comparing the van der Waals/non polar ($\ddot{A}E_{vdW}^{MM} + \ddot{A}G_{np}^{sol}$) and ($\ddot{A}E_{ele}^{MM} + \ddot{A}G_{ele}^{sol}$) contribution for all molecules reported. Indeed, the **5d-f**/helicase complexes formation paid a less penalty desolvation energy term than the **5h-j**/helicase assemblies, due to the presence of four apolar methyl groups. On the other hand, compounds **5a-c** are not able to optimize the intermolecular interactions within the helicase binding site, resulting in a looser fitting and in the presence of an intermittent formation of the H-bonds network. Accordingly, the corresponding $\ddot{A}E_{vdW}^{MM}$ terms in Table (**4**) are lower than those pertaining to compounds **5d-f**.

As discussed before, compounds **5d-f** exhibited good activity against both CVB-2 and Sb-1, while **5h-j** were found selective against CVB-2. This behavior can be explained, in the absence of a 3D model for the Coxsackie B2 helicase (see above), adopting a 2D alignment analysis. The putative binding site proposed for Sb-1 is composed by 30 residues and, according to our 2D alignment, the binding site for CVB-2 differs for 7 residues only. Among these, Ser296 in Sb-1 is mutated to Arg237 in CBV-2. Following our analysis, and a preliminary visual inspection based on the swapping of Ser to Arg in the Polio helicase (data not shown), we concluded that this is the most important residue in the case of compounds **5h-j**, featuring chlorine atoms as substituents. In fact, the positively charged side chain of Arg237 is placed at an average distance of 3.5 Å from the Cl atoms, thus sensibly resulting is strong electrostatic interactions between the inhibitor and the protein. These speculations, which may account in part for the selectivity of these compounds with respect to CVB-2, clearly await further confirmation from the simulations performed on the corresponding protein 3D models, which is currently under construction.

CONCLUSIONS

In the light of the above mentioned results, we conclude that *N,N'*-bis[4-(5,6-dimethyl-2*H*-benzotriazol-2-yl)phenyl]-alkyldicarboxamides (**5d-f**) are endowed with good activity against both Coxsackie B2 (CVB-2) and Polio (Sb-1), whereas *N,N'*-bis[4-(5,6-dichloro-2*H*-benzotriazol-2-yl)phenyl]alkyldicarboxamides (**5h-j**) emerged for their selective anti-CVB-2 activity and they might represent new interesting leads. Dimerization of the precedent monomeric series emerges as an important development for this class of helicase inhibitors.

Molecular modeling procedures adopted on title compounds/helicase Sb-1 complexes have shown to be able to rank binding affinities of all drugs, to provide insight into the interactions occurring in the active site, and the reasons of different activities in the corresponding binding free energy.

A preliminary, 2D qualitative analysis applied on inhibitors/helicase CVB-2 complexes has allowed us to uncover one of the possible origins of selectivity of compounds **5h-j** toward the Coxsackie B2 virus. Accordingly, the computational strategy used in this paper can provide a blueprint for new inhibitors in structure-based drug design or in predicting binding affinity of a ligand prior to new organic synthesis.

EXPERIMENTAL SECTION

Chemistry

M.p.s were uncorrected and were taken in open capillaries in a Digital Electrothermal IA9100 melting point apparatus. ^{1}H NMR spectra were recorded on a Varian XL-200 (200 MHz) instrument, using TMS as internal standard. The chemical shift values are reported in ppm (δ) and coupling constants (*J*) in Hertz (Hz). Signal multiplicities are represented by: s (singlet), d (doublet), dd (double doublet), m (multiplet). MS spectra were performed on a combined HP 5790 (GC)-HP 5970 (MS) apparatus or with a combined Liquid Chromatograph-Agilent 1100 series Mass Selective Detector (MSD). Column chromatography was performed using 70-230 mesh (Merck silica gel 60). The progress of the reactions, the R_f and the purity of the final compounds were monitored by TLC using Merck F-254 commercial plates. Analyses indicated by the symbols of the elements were within ± 0.4 % of the theoretical values.

Starting Materials and Intermediates

1-(4-Aminophenyl)benzotriazoles (**1a-d**), and 2-(4-aminophenyl)benzotriazoles (**4a-c**), were prepared following the procedure previously described by us [1], while 2-(4-aminophenyl)-5,6-dichlorobenzotriazole (**4d**) was prepared following the procedure below described.

N,N'-bis[4-(2-benzimidazolyl)phenyl]succinyldicarboxamides (III) was prepared following the procedure described by Diana *et al.* [2].

Succinoyl dichloride (**2a**), glutaryl dichloride (**2b**), adipoyl dichloride (**2c**), 4,5-dichloro-1,2-phenylendiamine (**6**) and 1-chloro-4-nitrobenzene (**8**) were commercially available (Aldrich).

Preparation of the Intermediates 1(2)-(4-aminophenyl)-5,6-dichlorobenzotriazole (1e and 4d)

i) A solution of sodium nitrite (2.0 g, 28 mmol) in water (10 mL) was added dropwise to a ice-cooled stirred solution of 4,5-dichloro-1,2-phenylendiamine (**6**) (2.5 g, 14.1 mmol) in 2 M hydrochloric aqueous solution (140 mL). After the addition was complete, the mixture was allowed to warm at r.t. and the stirring continued overnight. The resulting precipitate was filtered off obtaining 5,6-dichlorobenzotriazole (**7**) (2.45 g, 92 %), mp 262-264 (lit. 264-266 °C, [3]).

ii) To a stirred solution of **7**, (2.5 g, 13.3 mmol) and KOH (0.82 g, 15.3 mmol) in DMF (25 mL), a solution of 1-chloro-4-nitrobenzene (**8**) (2.09 g, 13.3 mmol) in DMF (6 mL), was slowly added dropwise. After then, the reaction mixture was heated at 100-110 °C and the stirring was continued for an additional 5 days. On cooling to r.t., a precipitate was filtered off, washed with water and dried, to give 3.19 g of the desired mixtures **9a**,**b** (78% yield).

iii) A solution of **9a**,**b** (1.0 g, 3.2 mmol) and methyl hydrazine (3 mL) in 120 mL of ethanol was heated in a sealed steel vessel at 100 °C for 80 h. The reaction mixture was then cooled to r.t. and the solvent was removed *in vacuo*. The crude solid was purified by chromatography on silica gel eluting with light petroleum-ethyl acetate in 7:3 ratio, to give in the sequence the desired **4d** (0.28 g) and **1e** (0.60 g). Melting points, yields, analytical and spectroscopical data are reported below.

2-(4-Aminophenyl)-5,6-dichlorobenzotriazole (4d)

This compound was obtained in 31 %; m.p. 238-240 °C (acetone); TLC (light petroleum-ethyl acetate 6:4): R_f 0.62; IR (nujol): ν 3410, 3350, 1604 cm^{-1}; UV (EtOH): λ_{max} 216, 360 nm; ^{1}H NMR ($CDCl_3$): δ 8.07 (dd, 2H, *J* = 9.0 and 2.2 Hz, H-2' + H-6'), 8.04 (s, 2H, H-4 + H-7), 6.80 (dd, 2H, *J* = 9.0 and 2.2 Hz, H-3' + H-5'). MS: *m/z* 278 (M^+); Anal. Calcd. for $C_{12}H_8Cl_2N_4$: C, 51.64; H, 2.89; N, 20.07. Found: C, 51.30, 2.60; N, 19.75.

1-(4-Aminophenyl)-5,6-dichlorobenzotriazole (1e)

This compound was obtained in 67 %; m.p. > 300 °C (acetone); TLC (light petroleum-ethyl acetate 6:4):R_f 0.44; IR (nujol): ν 3450, 3310, 1625 cm^{-1}; UV (EtOH): λ_{max} 213, 260, 345 nm; ^{1}H NMR ($CDCl_3$): δ 8.23 (s, 1H, H-4), 7.78 (s, 1H, H-7), 7.44 (dd, 2H, *J* = 8.6 and 2.0 Hz, H-2' + H-6'), 6.86 (dd, 2H, *J* = 8.6 and 2.0 Hz, H-3' + H-5'). MS: *m/z* 278 (M^+); Anal. Calcd. for $C_{12}H_8Cl_2N_4$: C, 51.64; H, 2.89; N, 20.07. Found: C, 51.26, 2.53; N, 19.69.

General Procedure for Preparation of *N*,*N*'-bis[4-(1*H*(2*H*)-benzotriazol-1(2)-yl)phenyl]alkyldicarboxamides (3a-f and 5a-j)

To a stirred solution of an equimolar amount of 1-(4-Aminophenyl)benzotriazoles (**1a-d**) or 2-(4-aminophenyl) benzotriazoles (**4a-c**) and TEA (2 mmol) in DMF (10 mL), a solution of the appropriate diacyl dichloride (**2a-c**) (1.1 mmol) in DMF (5 mL), was slowly added dropwise. After the addition was complete, the stirring was continued for an additional 3 h and, when the reaction was complete, the resulting precipitate of Et_3N,HCl was filtered and eliminated. The resulting mothers liquid were diluted with 100 mL of water, and the precipitate obtained was filtered off, washed with water, dried and crystallized with methanol, to afford the *bis*-benzotriazol-dicarboxamides (**3a-c** and **5a-c**) pure. In the case of the benzosubstituted derivatives (**3d-f** and **5d-j**), the solid crude obtained by dilution with water was purified by chromatography on silica gel (eluent: chloroform-methanol 8:2). Melting points, yields, analytical and spectroscopical data are reported below.

N,*N*'-bis[4-(1*H*-benzotriazol-1-yl)phenyl]succinylcarboxamide (3a)

This compound was obtained in 75% yield; m.p. > 300 °C (methanol); TLC (chloroform-methanol 9:1): R_f 0.63; IR (nujol): ν 3300, 1650, 1600 cm^{-1}; UV (EtOH): λ_{max} 205, 263, 296 nm; ^{1}H-NMR (DMSO-d_6): δ 10.42 (s, 2H, 2 NH), 8.18 (d, 2H, *J* = 8.0 Hz, 2 H-4), 7.95-7.84 (m, 6H, 2 H-7 + 2 H-2' + 2H-6'), 7.81 (d, 4H, *J* = 8.8 Hz, 2 H-3' + 2 H-5'), 7.66 (dd, 2H, *J* = 8.0 e 7.0 Hz, 2 H-6), 7.52 (dd, 2H, *J* = 8.0 e 7.0 Hz, 2 H-5), 2.78 (s, 4H, CH_2CH_2); LC/MS: 503 (100%) (M+H),

525 (M+Na); Anal. Calcd. for $C_{28}H_{22}N_8$: C, 66.92; H, 4.41; N, 22.30. Found: C, 66.58; H, 4.55; N, 22.21.

N,N'-bis[4-(1*H*-benzotriazol-1-yl)phenyl]glutarylcarboxamide (3b)

This compound was obtained in 77% yield; m.p. 233-235°C (methanol); TLC (chloroform-methanol 9:1): R_f 0.55; IR (nujol): ν 3300, 1670, 1605 cm^{-1}; UV (EtOH): λ_{max} 204, 263, 293 nm; ^{1}H-NMR ($CDCl_3$+DMSO-d_6): δ 10.12 (s, 2H, 2 NH), 8.10 (d, 2H, *J* = 8.2 Hz, 2 H-4), 7.96 (d, 4H, *J* = 8.8 Hz, 2 H-2' + 2 H-6'), 7.78 (d, 2H, *J* = 8.2 Hz, 2 H-7), 7.74 (d, 4H, *J* = 8.8 Hz, 2 H-3' + 2 H-5'), 7.60 (dd, 2H, *J* = 8.2 e 7.0 Hz, 2 H-6), 7.46 (dd, 2H, *J* = 8.2 e 7.0 Hz, 2 H-5), 2.58 (m, 4H, 2 COC*H*$_2$), 2,15 (m, 2H, $CH_2CH_2CH_2$); LC/MS: 517 (100%) (M+H), 539 (M+Na), 562 (M+2Na); Anal. Calcd. for $C_{29}H_{24}N_8$: C, 67.43; H, 4.68; N, 21.69. Found: C, 67.11; H, 4.80; N, 21.44.

N,N'-bis[4-(1*H*-benzotriazol-1-yl)phenyl]adipylcarboxamide (3c)

This compound was obtained in 46% yield; m.p. > 300 °C (methanol); TLC (chloroform-methanol 9:1): R_f 0.65; IR (nujol): ν 3300, 1655, 1600 cm^{-1}; UV (EtOH): λ_{max} 202, 283, 296 nm; ^{1}H-NMR ($CDCl_3$+DMSO-d_6): δ 10.17 (s, 2H, 2 NH), 8.11 (d, 2H, *J* = 8.2 Hz, 2 H-4), 7.94 (d, 4H, *J* = 8.8 Hz, 2 H-2' + 2 H-6'), 7.83 (d, 2H, *J* = 8.2 Hz, 2 H-7), 7.73 (d, 4H, *J* = 8.8 Hz, 2 H-3' + 2 H-5'), 7.61 (dd, 2H, *J* = 8.2 e 7.2 Hz, 2 H-6), 7.47 (dd, 2H, *J* = 8.2 e 7.0 Hz, 2 H-5), 2.46 (m, 4H, 2 COC*H*$_2$), 1.78 (m, 4H, $CH_2CH_2CH_2CH_2$); LC/MS: 531 (100%) (M+H); Anal. Calcd. for $C_{30}H_{26}N_8$: C, 67.91; H, 4.94; N, 21.12. Found: C, 68.18; H, 4.73; N, 21.49.

N,N'-bis[4-(5,6-dimethyl-1*H*-benzotriazol-1-yl)phenyl]succinylcarboxamide (3d)

This compound was obtained in 61% yield; m.p. 242-243°C (methanol); TLC (chloroform-methanol 8:2): R_f 0.51; IR (nujol): ν 3300, 1680, 1610 cm^{-1}; UV (EtOH): λ_{max} 204, 267, 298 nm; ^{1}H-NMR ($CDCl_3$ + DMSO-d_6): δ 10.14 (s, 2H, 2 NH), 7.91 (d, 4H, *J* = 8.8 Hz, 2 H-2' + 2 H-6'), 7.80 (s, 4H, 2 H-4 + 2 H-4), 7.66 (d, 4H, *J* = 8.8 Hz, 2 H-3' + 2 H-5'), 7.51 (s, 4H, 2 H-4 + 2 H-7), 2.69 (s, 4H, 2 CH_2), 2.44 (s, 12H, 2 C_5-C*H*$_3$ + 2 C_6-C*H*$_3$); LC/MS: 559 (20%) (M+H), 581 (M+Na); Anal. Calcd. for $C_{32}H_{30}N_8$: C, 68.8; H, 5.41; N, 20.06. Found: C, 69.17; H, 5.67; N, 19.81.

N,N'-bis[4-(5-trifluoromethyl-1*H*-benzotriazol-1-yl)phenyl]succinylcarboxamide (3e)

This compound was obtained in 20% yield; m.p. 280-281°C (methanol); TLC (dichloromethane-methanol 9:1): R_f 0.24; IR (nujol): ν 3100, 1640, 1610 cm^{-1}; UV (EtOH): λ_{max} 205, 260, 288 nm; ^{1}H-NMR ($CDCl_3$ + DMSO-d_6): δ 10.40 (s, 2H, 2 NH), 8.47 (s, 2H, 2 H-4), 8.01-7.81 (m, 10H, 2 H-6 + 2 H-2' + 2 H-3' + 2 H-5' + 2 H-6'), 7.71 (d, 2H, *J* = 8.8 Hz, 2 H-7), 2.65 (s, 4H, 2 CH_2); LC/MS: 639 (10%) (M+H), 661 (M+Na); Anal. Calcd. for $C_{30}H_{20}F_6N_8$: C, 56.43; H, 3.16; N, 17.55. Found: C, 56.08; H, 3.10; N, 17.88.

N,N'-bis[4-(6-trifluoromethyl-1*H*-benzotriazol-1-yl)phenyl]succinylcarboxamide (3f)

This compound was obtained in 15% yield; m.p. 287-288°C (methanol); TLC (dichloromethane-methanol 9:1): R_f 0.38; IR (nujol): ν 3200, 1680, 1600 cm^{-1}; UV (EtOH): λ_{max} 205, 256, 302 nm; ^{1}H-NMR ($CDCl_3$ + DMSO-d_6): δ 10.71 (s, 2H, 2 NH), 8.20 (d, 2H, *J* = 8.6 Hz, 2 H-5), 7.95 (d, 4H, *J* = 8.8 Hz, 2 H-2' + 2 H-6'), 7.69-7.63 (m, 4H, 2 H-4 + 2 H-7), 7.58 (d, 4H, *J* = 8.8 Hz, 2 H-3' + 2 H-5'), 2.59 (s, 4H, 2 CH_2); LC/MS: 639 (5%) (M+H); Anal. Calcd. for $C_{30}H_{20}F_6N_8$: C, 56.43; H, 3.16; N, 17.55. Found: C, 56.12; H, 2.98; N, 17.43.

N,N'-bis[4-(2*H*-benzotriazol-2-yl)phenyl]succinylcarboxamide (5a)

This compound was obtained in 78% yield; m.p. > 300 °C (methanol); TLC (chloroform-methanol 9:1): R_f 0.31; IR (nujol): ν 3300, 1700, 1650, 1600 cm^{-1}; UV (EtOH): λ_{max} 200, 253, 264, 328 nm; ^{1}H-NMR ($CDCl_3$ + DMSO-d_6): δ 10.36 (s, 2H, 2 NH), 8.25 (d, 4H, *J* = 9.0 Hz, 2 H-2' + 2 H-6'), 7.96 (m, 4H, 2 H-4 + 2 H-7), 7.89 (d, 4H, *J* = 9.0 Hz, 2 H-3' + 2 H-5'), 7.47 (m, 4H, 2 H-5 + 2 H-6), 2.78 (s, 4H, C*H*$_2$C*H*$_2$); LC/MS: 503 (100%) (M+H); Anal. Calcd. for $C_{28}H_{22}N_8$: C, 66.92; H, 4.41; N, 22.30. Found: C, 66.58; H, 4.55; N, 22.21.

N,N'-bis[4-(2*H*-benzotriazol-2-yl)phenyl]glutarylcarboxamide (5b)

This compound was obtained in 80% yield; m.p. > 300 °C (methanol); TLC (chloroform-methanol 9:1): R_f 0.75; IR (nujol): ν 3270, 1660, 1600 cm^{-1}; UV (EtOH): λ_{max} 202, 256, 264, 324 nm; ^{1}H-NMR ($CDCl_3$ + DMSO-d_6): δ 10.12 (s, 2H, 2 NH), 8.24 (d, 4H, *J* = 9.0 Hz, 2 H-2' + 2 H-6'), 7.95-7.87 (m, 8H, 2 H-4 + 2 H-7 + 2 H-3' + 2 H-5'), 7.47 (m, 4H, 2 H-5 + 2 H-6), 2.56 (m, 4H, 2 COC*H*$_2$), 2,15 (m, 2H, $CH_2CH_2CH_2$); LC/MS: 517 (100%) (M+H); Anal. Calcd. for $C_{29}H_{24}N_8$: C, 67.43; H, 4.68; N, 21.69. Found: C, 67.07; H, 4.35; N, 21.31.

N,N'-bis[4-(2*H*-benzotriazol-2-yl)phenyl]adipylcarboxamide (5c)

This compound was obtained in 46% yield; m.p. 224-226 °C (methanol); TLC (chloroform-methanol 9:1): R_f 0.38; IR (nujol): ν 3300, 1700, 1650, 1600 cm^{-1}; UV (EtOH): λ_{max} 203, 255, 264, 324 nm; ^{1}H-NMR (DMSO-d_6): δ 10.27 (s, 2H, 2 NH), 8.26 (d, 4H, *J* = 9.0 Hz, 2 H-2' + 2 H-6'), 8.02 (m, 4H, 2 H-4 + 2 H-7), 7.87 (d, 4H, *J* = 9.0 Hz, 2 H-3' + 2 H-5'), 7.52 (m, 4H, 2 H-5 + 2 H-6), 2.35 (m, 4H, 2 COC*H*$_2$), 1.62 (m, 4H, $CH_2CH_2CH_2CH_2$); LC/MS: 531 (100%) (M+H); Anal. Calcd. for $C_{30}H_{26}N_8$: C, 67.91; H, 4.94; N, 21.12. Found: C, 67.59; H, 5.06; N, 21.01.

N,N'-bis[4-(5,6-dimethyl-2*H*-benzotriazol-2-yl)phenyl]succinylcarboxamide (5d)

This compound was obtained in 58% yield; m.p. > 300 °C (methanol); TLC (chloroform-methanol 8:2): R_f 0.49; IR (nujol): ν 3300, 1700, 1660, 1600 cm^{-1}; UV (EtOH): λ_{max} 202, 260, 329 nm; 1H-NMR (CDCl3 + DMSO-d6): δ 10.27 (s, 2H, 2 NH), 8.18 (d, 4H, *J* = 8.8 Hz, 2 H-2' + 2 H-6'), 7.83 (d, 4H, *J* = 8.8 Hz, 2 H-3' + 2 H-5'), 7.66 (s, 4H, 2 H-4 + 2 H-7), 2.56 (s, 4H, 2 CH2), 2.42 (s, 12H, 2 C5-C*H*3 + 2 C6-C*H*3); LC/MS: 559 (10%) (M+H); Anal. Calcd. for $C_{32}H_{30}N_8$: C, 68.80; H, 5.41; N, 20.06. Found: C, 68.61; H, 5.65; N, 19.70.

N,N'-bis[4-(5,6-dimethyl-2*H*-benzotriazol-2-yl)phenyl]glutarylcarboxamide (5e)

This compound was obtained in 45% yield; m.p. > 300 °C (methanol); TLC (chloroform-methanol 9:1): R_f 0.33; IR (nujol): ν 3300, 1690, 1655, 1600 cm^{-1}; UV (EtOH): λ_{max} 202, 265, 327 nm; ^{1}H-NMR ($CDCl_3$ + DMSO-d_6): δ 10.01 (s, 2H, 2 NH), 8.18 (d, 4H, *J* = 8.8 Hz, 2 H-2' + 2 H-6'), 7.85 (d, 4H, *J* = 8.8 Hz, 2 H-3' + 2 H-5'), 7.63 (m, 4H, 2 H-4 + 2 H-7), 2.59 (m, 4H, 2 $COCH_2$), 2.42 (s, 12H, 2 C_5-CH_3 + 2 C_6-CH_3), 1.98 (m, 2H, $CH_2CH_2CH_2$); LC/MS: 573 (20%) (M+H); Anal. Calcd. for $C_{33}H_{32}N_8$: C, 69.21; H, 5.63; N, 19.57. Found: C, 68.82; H, 5.80; N, 19.19.

N,N'-bis[4-(5,6-dimethyl-2*H*-benzotriazol-2-yl)phenyl]adipylcarboxamide (5f)

This compound was obtained in 40% yield; m.p. > 300 °C (methanol); TLC (chloroform-methanol 9:1): R_f 0.42; IR (nujol): ν 3300, 1685, 1650, 1600 cm^{-1}; UV (EtOH): λ_{max} 203, 260, 320 nm; ^{1}H-NMR (DMSO-d_6): δ 10.15 (s, 2H, 2 NH), 8.18 (d, 4H, *J* = 8.6 Hz, 2 H-2' + 2 H-6'), 7.83 (d, 4H, *J* = 8.6 Hz, 2 H-3' + 2 H-5'), 7.63 (s, 2H, 2 H-4 + 2 H-7), 2.52 (m, 4H, 2 $COCH_2$), 2.45 (s, 12H, 2 C_5-CH_3 + 2 C_6-CH_3), 1.70 (m, 4H, $CH_2CH_2CH_2CH_2$); LC/MS: 587 (15%) (M+H); Anal. Calcd. for $C_{34}H_{34}N_8$: C, 69.61; H, 5.84; N, 19.10. Found: C, 69.73; H, 5.80; N, 18.70.

N,N'-bis[4-(5-trifluoromethyl-2*H*-benzotriazol-2-yl)phenyl]succinylcarboxamide (5g)

This compound was obtained in 57% yield; m.p. 265-267°C (methanol); TLC (dichloromethane-methanol 9:1): R_f 0.63; IR (nujol): ν 3290, 1650 cm^{-1}; UV (EtOH): λ_{max} 210, 266, 332 nm; ^{1}H-NMR ($CDCl_3$ + DMSO-d_6): δ 10.34 (s, 2H, 2 NH), 8.34 (s, 2H, H-4), 8.24 (d, 2H, *J* = 8.8 Hz, 2 H-6), 8.06 (d, 4H, *J* = 8.8 Hz, 2 H-2' + 2 H-6'), 7.84 (d, 2H, *J* = 8.8 Hz, 2 H-7), 7.62 (d, 4H, *J* = 8.8 Hz, 2 H-3' + 2 H-5'), 2.56 (s, 4H, 2 CH_2); LC/MS: 639 (17%) (M+H); Anal. Calcd. for $C_{30}H_{20}F_6N_8$: C, 56.43; H, 3.16; N, 17.55. Found: C, 56.80; H, 3.31; N, 17.09.

N,N'-bis[4-(5,6-dichloro-2*H*-benzotriazol-2-yl)phenyl]succinylcarboxamide (5h)

This compound was obtained in 15 % yield; m.p. > 300 °C (methanol); TLC (chloroform-methanol 9:1): R_f 0.16; IR (nujol): ν 3313, 1727, 1642, 1606 cm^{-1}; UV (EtOH): λ_{max} 210, 342 nm; ^{1}H-NMR ($CDCl_3$ + DMSO-d_6): δ 10.37 (s, 2H, 2 NH), 8.43 (s, 4H, 2 H-4 + 2 H-7), 8.23 (d, 4H, *J* = 9.0 Hz, 2 H-2' + 2 H-6'), 7.93 (d, 4H, *J* = 9.0 Hz, 2 H-3' + 2 H-5'), 2.56 (m, 4H, 2 CH_2); LC/MS: 639 (15 %) (M+H); Anal. Calcd. for $C_{28}H_{18}Cl_4N_8$: C, 52.52; H, 2.83; N, 17.50. Found: C, 52.07; H, 3.01; N, 17.31.

N,N'-bis[4-(5,6-dichloro-2*H*-benzotriazol-2-yl)phenyl]glutarylcarboxamide (5i)

This compound was obtained in 30 % yield; m.p. > 300 °C (methanol); TLC (chloroform-methanol 9:1): R_f 0.18; IR (nujol): ν 3293, 1698, 1658, 1597 cm^{-1}; UV (EtOH): λ_{max} 210, 342 nm; ^{1}H-NMR ($CDCl_3$ + DMSO-d_6): δ 10.38 (s, 2H, 2 NH), 8.36 (s, 4H, 2 H-4 + 2 H-7), 8.22 (d, 4H, *J* = 8.6 Hz, 2 H-2' + 2 H-6'), 7.90 (d, 4H, *J* = 8.6 Hz, 2 H-3' + 2 H-5'), 2.57 (m, 4H, 2 $COCH_2$), 1.92 (m, 2H, $CH_2CH_2CH_2$); LC/MS: 653 (20%) (M+H); Anal. Calcd. for $C_{29}H_{20}Cl_4N_8$: C, 53.23; H, 3.08; N, 17.12. Found: C, 53.59; H, 3.22; N, 17.50.

N,N'-bis[4-(5,6-dichloro-2*H*-benzotriazol-2-yl)phenyl]adipylcarboxamide (5j)

This compound was obtained in 18 % yield; m.p. > 300 °C (methanol); TLC (chloroform-methanol 9:1): R_f 0.29; IR (nujol): ν 3284, 1654, 1595 cm^{-1}; UV (EtOH): λ_{max} 212, 342 nm; ^{1}H-NMR (DMSO-d_6): δ 10.40 (s, 2H, 2 NH), 8.40 (s, 2H, 2 H-4 + 2 H-7), 8.25 (d, 4H, *J* = 8.6 Hz, 2 H-2' + 2 H-6'), 7.91 (d, 4H, *J* = 8.6 Hz, 2 H-3' + 2 H-5'), 2.94 (m, 4H, 2 $COCH_2$), 1.18 (m, 4H, $CH_2CH_2CH_2CH_2$); LC/MS: 667 (15%) (M+H), Anal. Calcd. for $C_{30}H_{22}Cl_4N_8$: C, 53.91; H, 3.32; N, 16.77. Found: C, 54.29; H, 3.12; N, 17.08.

Cell-Based Assays

Compounds

Compounds were dissolved in DMSO at 100 mM and then diluted in culture medium.

Cells and Viruses

Cell lines were purchased from American Type Culture Collection (ATCC). The absence of mycoplasma contamination was checked periodically by the Hoechst staining method. Cell lines supporting the multiplication of RNA viruses were the following: Madin Darby Bovine Kidney (MDBK); Baby Hamster Kidney (BHK-21); Monkey kidney (Vero 76) and $CD4^+$ human T-cells containing an integrated HTLV-1 genome (MT-4).

Cytotoxicity Assays

For cytotoxicity tests, run in parallel with antiviral assays, MDBK, BHK and Vero 76 cells were resuspended in 96 multiwell plates at an initial density of $6x10^5$, $1x10^6$ and $5x10^5$ cells/mL, respectively, in maintenance medium, without or with serial dilutions of test compounds. Cell viability was determined after 48-96 hrs at 37 °C in a humidified CO_2 (5%) atmosphere by the 3-(4,5-dimethylthiazol-2-yl)-2,5-diphenyltetrazolium bromide (MTT) method [4]. The cell number of Vero 76 monolayers was determined by staining with the methylene blue dye.

For cytotoxicity evaluations, exponentially growing cells derived from human haematological tumors [$CD4^+$ human T-cells containing an integrated HTLV-1 genome (MT-4)] were seeded at an initial density of $1x10^5$ cells/mL in 96 well plates in RPMI-1640 medium supplemented with 10% fetal calf serum (FCS), 100 units/mL penicillin G and 100 µg/mL streptomycin. Cell cultures were then incubated at 37 °C in a humidified, 5% CO_2 atmosphere in the absence or presence of serial dilutions of test compounds. Cell viability was determined after 96 hrs at 37 °C by the MTT method.

Antiviral Assays

Activity of compounds against Yellow fever virus (YFV) and Bovine viral diarrhoea virus (BVDV) were based on inhibition of virus-induced cytopathogenicity in acutely infected BHK-21 and MDBK cells, respectively.

BHK and MDBK cells were seeded in 96-well plates at a density of $5x10^4$ and $3x10^4$ cells/well, respectively, and were

allowed to form confluent monolayers by incubating overnight in growth medium at 37 °C in a humidified CO_2 (5%) atmosphere. Cell monolayers were then infected with 50 μL of a proper virus dilution (in serum-free medium) to give an m.o.i = 0.01. 1 hr later, 50 μL of MEM Earle's medium, supplemented with inactivated foetal calf serum (FCS), 1% final concentration, without or with serial dilutions of test compounds, were added. After a 3 day incubation at 37 °C, cell viability was determined by the MTT method.

Activity of compounds against Coxsackie virus, B-2 strain (CVB-2), Polio virus type-1 (Polio-1), Sabin strain, was determined by plaque reduction assays in Vero 76 cell monolayers. To this end, Vero 76 cells were seeded in 24-well plates at a density of $2.5x10^5$ cells/well and were allowed to form confluent monolayers by incubating overnight in growth medium at 37 °C in a humidified CO_2 (5%) atmosphere. Then, monolayers were infected with 250 μL of proper virus dilutions to give 50-100 PFU/well. Following removal of unadsorbed virus, 500 μL of Dulbecco's modified Eagle's medium, supplemented with 1% inactivated FCS and 0.75% methyl cellulose, without or with serial dilutions of test compounds, were added. Cultures were incubated at 37 °C for 2 (Sb-1), 3 (CVB-2) days and then fixed with PBS containing 50% ethanol and 0.8% crystal violet, washed and air-dried. Plaques were then counted. 50% effective concentrations (EC_{50}) were calculated by linear regression technique.

Molecular Modeling

The 3D model structure of the Polio (Sb-1) helicase, presently not available in Protein Data Bank (PDB), was built by a combination of homology-based techniques [5,1]. Accordingly, we only report here a brief explanation of the procedure adopted. The *Modeller* program [6,7] was employed to build a preliminary 3D model of the enzyme (reference structure PDB entry code 1SQ5, chain A [8]). The complete 3D model structure of the Polio helicase obtained with our procedure was refined by several, gradual energy minimization rounds. The *Amber* 7.0 software [9] with the Cornell et al. (*parm94*) parameter set [10] was used to this purpose. The quality of the model was assessed by using different validation tools [11,12]. Ramachandran plot statistics indicated that 94% of the main-chain dihedral angles were found in the most favourable region, thus confirming the good quality of the 3D model of the Polio helicase obtained. This optimized 3D model was then used as the entry point for molecular dynamics (MD) simulations. The putative binding site of title compounds on the Polio helicase was determined using the *ActiveSite_Search* option of the *Binding Site* module of *InsightII* (v. 2001, Accelrys, San Diego, USA). *ActiveSite_Search* identifies protein active sites or binding sites by locating cavities in the protein structure. According to the Site Search algorithm employed, the protein is first mapped onto a grid which covers the complete protein space. The grid points are then defined as free points and protein points. The protein points are grid points, within 2 Å from a hydrogen atom or 2.5 Å from a heavy atom. Then, a cubic eraser moves from the outside of the protein toward the center to remove the free points until the opening is too small for it to move forward. Those free points not reached by the eraser will be defined as site points. After a site is located, it can be modified by expanding or contracting the site. One layer of grid points at the cavity opening site will be added or removed by each expand or contract operation, respectively.

The model structures of title compounds were generated using the *Biopolymer* module of Insight II. All molecules were subjected to an initial energy minimization, again using the sander module of the *Amber* 7.0 suite of programs, with the parm94 version of the Amber field. The convergence criterion was set to 10-4 kcal/(mol Å). A conformational search was carried out using a well-validated combined molecular mechanics/molecular dynamics simulated annealing (MDSA) protocol [13-16]. Accordingly, the relaxed structures were subjected to 5 repeated temperature cycles (from 298 K to 1000 K and back) using constant volume/constant temperature (NVT) MD conditions. At the end of each annealing cycle, the structures were again energy minimized to converge below 10^{-4} kcal/(mol Å), and only the structures corresponding to the minimum energy were used for further modeling. The atomic partial charges for the geometrically optimized compounds were obtained using the RESP procedure [17], and the electrostatic potentials were produced by single-point quantum mechanical calculations at the Hartree-Fock level with a 6-31G* basis set, using the Merz-Singh-Kollman van der Waals parameters [18].

The optimized structures of all compounds were docked into the putative Polio helicase binding site following to a validated procedure [14,16,19]; accordingly, it will be described here only briefly. The software *AutoDock* 3.0 [20] was employed to estimate the possible binding orientations of all compounds in the receptor. In order to encase a reasonable region of the protein surface and interior volume, centered on the identified binding site, the grids were 40 Å on each side. Grid spacing (0.375 Å), and 80 grid points were applied in each Cartesian direction so as to calculate mass-centered grid maps. Amber 12-6 and 12-10 Lennard-Jones parameters were used in modeling van der Waals interactions and hydrogen bonding (N-H, O-H and S-H), respectively. In the generation of the electrostatic grid maps, the distance dependent relative permittivity of Mehler and Solmajer [21] was applied.

For the docking of each compound to the protein, three hundred Monte Carlo/Simulated Annealing (MC/SA) runs were performed, with 100 constant temperature cycles for simulated annealing. For these calculations, the GB/SA implicit water model [22] was used to mimic the solvated environment. The rotation of the angles φ and ψ, and the angles of side chains were set free during the calculations. All other parameters of the MC/SA algorithm were kept as default. Following the docking procedure, all structures of compounds were subjected to cluster analysis with a tolerance of 1 Å for an all-atom root-mean-square (RMS) deviation from a lower-energy structure representing each cluster family. In the absence of any relevant crystallographic information, the structure of each resulting complex characterized by the lowest interaction energy was selected for further evaluation.

Each best substrate/helicase complex resulting from the automated docking procedure was further refined in the Amber suite using the quenched molecular dynamics method

(QMD) [23]. In this case, 100 ps MD simulation at 298 K were employed to sample the conformational space of the substrate-enzyme complex in the GB/SA continuum solvation environment [22]. The integration step was equal to 1 fs. After each ps, the system was cooled to 0 K, the structure was extensively minimized, and stored. To prevent global conformational changes of the enzyme, the backbone of the protein binding site were constrained by a harmonic force constant of 100 kcal/Å, whereas the amino acid side chains and the ligands were allowed moving without any constraint.

The best energy configuration of each complex resulting from the previous step was solvated by adding a sphere of TIP3P water molecules [24] with a 30 Å radius from the mass center of the ligand with the use of the cap option of the leap module of Amber 7.0. The protein complex was neutralized adding a suitable number of counterions (Na+ and Cl-) in the positions of largest electrostatic potential, as determined by the module *Cion* of the Amber platform. The counterions, which had distances larger than 25 Å from the active site, were fixed in space during all simulations to avoid artifactual long range electrostatic effects on the calculated free energies. After energy minimization of the water molecules for 1500 steps, and MD equilibration of the water sphere with fixed solute for 20 ps, further unfavorable interactions within the structures were relieved by progressively smaller positional restraints on the solute (from 25 to 0 kcal/(mol Å2) for a total of 4000 steps. Each system was gradually heated to 298 K in three intervals, allowing a 5 ps interval per each 100 K, and then equilibrated for 50 ps at 298 K, followed by 400 ps of data collection runs, necessary for the estimation of the free energy of binding (vide infra). After the first 20 ps of MD equilibration, additional TIP3P water molecules were added to the 30 Å water cap to compensate for those who were able to diffuse into gaps of the enzyme. The MD simulations were performed at 298 K using the Berendsen coupling algorithm [25], an integration time step of 2 fs, and the applications of the shake algorithm [26] to constrain all bonds to their equilibrium values, thus removing high frequency vibrations. Long-range nonbonded interactions were truncated by using a 30 Å residue-based cut-off. For the calculation of the binding free energy between Polio helicase and title compounds in water, a total of 400 snapshots were saved during the MD data collection period described above, one snapshot per each 1 ps of MD simulation. The binding free energy ΔG_{bind} of each complex in water was calculated according to the procedure termed MM/PBSA (Molecular Mechanic/Poisson-Boltzmann Surface Area) and proposed by Srinivasan et al. [27]. Since the theoretical background of this methodology is described in details in the original paper, it will be only briefly described below. Following the MM/PBSA theory, the binding free energy between a given title compound and the target enzyme can be calculated as:

$$\Delta G_{bind} = \Delta E_{MM} + \Delta G_{solv} - T\Delta S \quad (1)$$

where:

$$\Delta G_{solv} = \ddot{A}G^{sol}_{ele} + \ddot{A}G^{sol}_{np} \quad (2)$$

ΔE_{MM} denotes the sum of molecular mechanics (MM) energies of the molecules, and can be further split into contributions from electrostatic ($\ddot{A}E^{MM}_{ele}$) and van der Waals ($\ddot{A}E^{MM}_{vdW}$) energies: Ä

$$\Delta E_{MM} = \ddot{A}E^{MM}_{ele} + \ddot{A}E^{MM}_{vdW} \quad (3)$$

The terms in equation (3) were calculated by using the carnal and anal modules of Amber 7.0. ΔG_{solv} represents the solvation free energy. The polar solvation process (i.e., $\ddot{A}G^{sol}_{ele}$ in eq. (2)) is equivalent to the transfer of a protein from one medium with dielectric constant equal to that of the interior of the protein to another medium with dielectric constant equal to that of the exterior of the protein. This term yields a free energy because it corresponds to the work done to reversibly charge the solute, and it is a polarization free energy because the work goes to the polarization of the solvent. The non polar solvation contribution (i.e., $\ddot{A}G^{sol}_{np}$ in eq. (2)) includes cavity creation in water and van der Waals interactions between the modeled nonpolar protein and water molecules. This term can be imagined as transferring a nonpolar molecule with the shape of the protein from vacuum to water. The polar component of ΔG_{solv} was evaluated with the Poisson-Boltzmann (PB) approach [28]. This procedure involves using a continuum solvent model, which represents the solute as a low dielectric medium (i.e. of dielectric constant $\varepsilon = 1$) with embedded charges and the solvent as a high dielectric medium ($\varepsilon = 80$) with no salt. All atomic charges were taken from the Cornell et al. force field and from our ab initio calculations (see above), since these are consistent with the MM energy calculations. The dielectric boundary is the contact surface between the radii of the solute and the radius (1.4 Å) of a water molecule. The numerical solution of the linearized Poisson-Boltzmann equations were solved on a cubic lattice by using the iterative finite-difference method implemented in the DelPhi software package [29]. The grid size used was 0.5 Å. Potentials at the boundaries of the finite-difference lattice were set to the sum of the Debye-Hückel potentials. The non-polar contribution to the solvation energy was calculated as $\Delta GNP = \gamma (SASA) + \beta$, in which $\gamma = 0.00542$ kcal/Å2, $\beta = 0.92$ kcal/mol, and SASA is the solvent-accessible surface estimated with the MSMS program [30].

The normal-mode analysis approach was followed to estimate the last parameter, i.e. the change in solute entropy upon association $-T\Delta S$ [31]. In the first step of this calculation, an 8-Å sphere around each title compound was cut out from an MD snapshot for each inhibitor-protein complex. This value was shown to be large enough to yield converged mean changes in solute entropy. On the basis of the size-reduced snapshots of the complex, we generated structures of the uncomplexed reactants by removing the atoms of the protein and ligand, respectively. Each of those structures was minimized, using a distance-dependent dielectric constant $\varepsilon = 4r$, to account for solvent screening, and its entropy was calculated using classical statistical formulas and normal mode-analysis. To minimize the effects due to different conformations adopted by individual snapshots we averaged the estimation of entropy over 10 snapshots.

ACKNOWLEDGEMENTS

This work was supported by grants from Italian [FIRB (RBNE01J3SK 001)] and European [VIZIER (LSHGCT-2004-511960)] Projects.

REFERENCES

[1] Carta, A.; Loriga, M.; Piras, S.; Paglietti, G.; La Colla, P.; Collu, G.; Piano, M. A.; Loddo, R. *Med. Chem.,* **2006**, *2*, 577.
[2] Diana, G.D.; Bailey, T.R. **1997** US patent, 5633388.
[3] Wiley, R.H.; Hssung, K.F. *J. Am. Chem. Soc*., 1957, 79, 4395-4399.
[4] Pauwels, R.; Balzarini, J.; Baba, M.; Snoeck, R.; Schols, D.; Herdewijn, P.; Desmyster, J.; De Clercq, E. *J. Virol. Methods*, **1988**, *20*, 309.
[5] Marti-Renom, M.A.; Stuart, A.C.; Fiser, A.; Sánchez, R.; Melo, F.; Sali, A. *Annu. Rev. Biophys. Biomol. Struct*., **2000**, *29*, 291.
[6] Sali, A.; Blundell, T.L. *J. Mol Biol*., **1993**, *234*, 779.
[7] Sali, A.; Potterton, L.; Yuan, F.; van Vlijmen, H.; Karplus, M. *Proteins*, **1995**, *23*, 318.
[8] Ivey, R.A.; Zhang, Y.M.; Virga, K.G.; Hevener, K.; Lee, R.E.; Rock, C.O.; Jackowski, S.; Park, H.W. *J. Biol. Chem*., **2004**; *279*, 35622.
[9] Case, D.A.; Pearlman, D.A.; Caldwell, J.D.; Cheatham III, T.E.; Wang, J.; Ross, W.S.; Simmerling, C.; Darden, T.A.; Merz, K.M.; Stanton, R.V.; Cheng, A.L.; Vincent, J.J.; Crowley, M.; Tsui, V.; Gohlke, H.; Radmer, R.J.; Duan, Y.; Pitera, J.; Massova, I.; Seibel, G.L.; Singh, U.C.; Weiner, P.K.; Kollman, P.A. AMBER 7 University of California, San Francisco, CA, USA, **2002**.
[10] Cornell, W.D.; Cieplak, P.;. Bayley, C.I; Gould, I.; Merz, K.M.; Ferguson, D.M.; Spellmeyer, D.C.; Fox, T.; Caldwell, J.W.; Kollman, P.A. *J. Am. Chem. Soc*., **1995**, *117*, 5179.
[11] Laskowski, R.A.; MacArthur, M.W.; Moss, D.S.; Thornton, J.M. *J. Appl. Crys*., **1993**; *26*, 283.
[12] Rhodriguez, R.; Chinea, G.; Lopez, N.; Pons, T.; Vriend, G. *CABIOS*, **1998**, *14*, 523.
[13] Fermeglia, M.; Ferrone, M.; Pricl, S. *Bioorg. Med. Chem*., **2002**, *10*, 2471.
[14] Felluga, F.; Pitacco, G.; Valentin, E.; Coslanich, A.; Fermeglia, M.; Ferrone, M.; Pricl, S.; *Tetrahedron: Asymmetry*, **2003**, *14*, 3385.
[15] Manfredini, S.; Solaroli, N.; Angusti, A.; Nalin, F.; Durini, E.; Vertuani, S.; Pricl, S.; Ferrone, M.; Spadari, S.; Focher, F.; Verri, A.; De Clercq, E.; Balzarini, J. *J. Antivir. Chem. Chemother.*, **2003**, *14*, 183.
[16] Mamolo, M.G.; Zampieri, D.; Vio, L.; Fermeglia, M.; Ferrone, M.; Pricl, S.; Scialino, G.; Banfi, E. *Bioorg. Med. Chem*., **2005**, *13*, 3797.
[17] Bayly, C.I.; Cieplak, P.; Cornell, W.D.; Kollman, P.A. *J. Phys. Chem*., **1993**, *97*, 10269.
[18] Besler, B.H.; Merz, K.M.; Kollman, P.A. *J. Comput. Chem*., **1990**, *11*, 431.
[19] Felluga, F.; Fermeglia, M.; Ferrone, M.; Pitacco, G.; Pricl, S.; Valentin, E. *Tetrahedron: Asymmetry*, **2002**, *13*, 475.
[20] Morris, G.M.; Goodsell, D.S.; Halliday, R.S.; Huey, R.; Hart, W.E.; Belew, R.K.; Olson, A.J. *J. Comput. Chem.*, **1998**, *19*, 1639.
[21] Mehler, E.L.; Solmajer, T. *Protein Eng*., **1991**, *4*, 903.
[22] Jayaram, B.; Sprous, D.; Beveridge, D.L. *J. Phys. Chem. B*, **1998**, *102*, 9571.
[23] Frecer, V.; Kabelac, M.; De Nardi, P.; Pricl, S.; Miertus, S. *J. Mol. Graph. Model*, **2004**, *22*, 209.
[24] Jorgensen, W.L.; Chandrasekhar, J.; Madura, J.D.; Impey, R.W.; Klein, M.L. *J. Comput. Phys*., **1983**, *79*, 926.
[25] Berendsen, H.J.C.; Postma, J.P.M.; van Gunsteren, W.F.; DiNola, A.; Haak, J.R. *J. Comput. Phys*., **1984**, *81*, 3684.
[26] Ryckaert, J.P.; Ciccotti, G.; Berendsen, H.J.C. *Comput. Phys*., **1977**, *23*, 327.
[27] Srinivasan, J.; Cheatham III, T.E.; Cieplak, P.; Kollman, P.A.; Case, D.A. *J. Am. Chem. Soc.*, **1998**, *120*, 9401.
[28] Gilson, M.K.; Sharp, K.A.; Honig, B.H. *J. Comput. Chem*., **1987**, *9*, 327.
[29] Sitkoff, D.; Sharp, K.A.; Honig, B.H. *J. Phys. Chem*., **1994**, *98*, 1978.
[30] Sanner, M.F.; Olson, A.J.; Spehner, J.C. *Biopolymers*, **1996**, *38*, 305.
[31] Wilson, E.B.; Decius, J.C.; Cross, P.C. *Molecular Vibrations*; McGraw-Hill: New York, **1955**.

Received: 29 September, 2006 **Revised: 29 January, 2007** **Accepted: 31 January, 2007**